Metachronal waves formation in 3D cilia arrays immersed in a two-phase flow

S. CHATEAU[a, b], S. PONCET[a, b], J. FAVIER[b], U. D'ORTONA[b]

a. Département de génie mécanique, Université de Sherbrooke, Sherbrooke, Québec, Canada.
sylvain.chateau@USherbrooke.ca & sebastien.poncet@USherbrooke.ca
b. Aix Marseille Université, CNRS, Centrale Marseille, Laboratoire M2P2 UMR 7340, Marseille, France.
julien.favier@univ-amu.fr & umberto.d-ortona@univ-amu.fr

Résumé :

Dans ce travail, la méthode Lattice Boltzmann couplée à la méthode des frontières immergées est utilisée pour étudier l'émergence d'ondes métachronales antipleptiques et symplectiques dans des rangées 3D de cils immergés dans un environnement diphasique, avec un rapport de viscosité de 20. La couche de fluide périciliaire (PCL) est confinée entre la surface épithéliale et la couche de mucus. Sa profondeur est choisie de telle sorte que le bout des cils puisse pénétrer dans la couche de mucus. Une rétroaction d'origine hydrodynamique est prise en compte à travers un paramètre de couplage α. Une étude comparative des ondes symplectiques et antipleptiques est également effectuée. Les ondes antipleptiques se révèlent être systématiquement plus performantes que les ondes symplectiques pour transporter et mélanger les fluides.

Abstract :

In the present work, the formation of antipleptic and symplectic metachronal waves in 3D cilia arrays immersed in a two-fluid environment, with a viscosity ratio of 20, is reported. A coupled lattice-Boltzmann - Immersed-Boundary solver is used. The periciliary layer (PCL) is confined between the epithelial surface and the mucus. Its thickness is chosen such that the tips of the cilia can penetrate the mucus. A hydrodynamical feedback of the fluids is taken into account through a coupling parameter α. A comparative study of both antipleptic and symplectic waves is also performed. The antipleptic waves are found to systematically outperform symplectic waves for transporting and mixing the fluids.

Keywords : Lattice-Boltzmann method, Immersed Boundary, Metachronal waves, Mucociliary clearance

1. Introduction

Ciliary propulsion is a universal phenomenon developed by nature as a way to propel fluids. It can be found in almost every living organisms, going from the prokaryotic bacteria to mammals. In the

particular case of the mucociliary clearance, cilia are found in tufts and serve to propel the mucus, a complex fluid whose purpose is to protect the bronchial epithelium against foreign particles.

This epithelium is covered by a fluid layer called the Airways Surface Liquid (ASL), usually considered to be the superposition of two layers : the periciliary liquid (PCL) and the mucus just above it. The PCL is generally considered to be a Newtonian fluid similar to water. In normal epithelium, its depth is around 6 μm, which allows the tips of the cilia (length of 7 μm) to emerge into the mucus layer. The mucus is a highly non-Newtonian fluid which possesses characteristics such as visco-elasticity and thixotropy [3]. Its height varies between 5 to 100 μm [1]. The main purpose of the mucus is to act as a barrier against the foreign particles that may enter the human body (dust, pollutants, bacteria) by catching them. The cilia protrude on the epithelial surface and serve to transport the mucus up to the stomach, where it can be digested. Their motion can be decomposed into two steps : the stroke and the recovery phases, which take around 1/3 and 2/3 of the beating period respectively. Their beating frequency varies between 10 and 20 Hz. Note that in creeping flows, only the spatial asymmetry is essential for the cilia to generate propulsion [4]. Defects in the mucociliary process usually lead to stagnant mucus, which induces breathing difficulties. Infections that may cause death also develop. It is then of prime importance to understand the hidden mechanisms behind the mucociliary clearance which allow thousands of cilia to act together for transporting mucus.

Indeed, early experimental observations [6] have shown that cilia do not usually beat randomly, but instead adapt their beatings accordingly to their neighbors, giving birth to metachronal waves (MCW). If the phase lag $\Delta\Phi$ between two cilia is positive ($0 < \Delta\Phi < \pi$), then the waves are called antipleptic MCW and move in the same direction as the fluid. On the contrary, if the phase lag $\Delta\Phi$ between two cilia is negative ($-\pi < \Delta\Phi < 0$), then the waves are called symplectic MCW and move in the opposite direction. For the particular case where $\Delta\Phi = 0$, the cilia beat synchronously, and for $\Delta\Phi = \pi$ a standing wave appears.

In this work, the formation of MCW is studied in a two-layer environment. To the best of our knowledge, the present study is the first one where both antipleptic and symplectic MCW are seen to emerge using a simple feedback law, while usually only one type of wave is observed, as in [14]. Moreover, while many studies considered single-layer fluid [15], only few had considered two-layer environments when studying MCW [16]. A parametric study where the metachrony is imposed is also performed. A particular value of phase lag $\Delta\Phi = \pi/4$, corresponding to an antipleptic MCW, is shown to be the more suitable for transporting and mixing the fluids. Finally, the numerical method possesses the following advantages : (i) viscosity ratios up to $O(10^2)$ can be achieved [10], and (ii) the mucus-PCL interface emerges intrinsically from the model. This solver is the only one that combines all these capabilities.

2. Numerical method

2.1 Geometrical modeling

The computational domain is a box composed of $N_x \times N_y \times N_z$ points regularly spaced. The cilia are hair-like structures modeled by a set of 20 Lagrangian points, such that their base point is located at $z = 0$ along the wall. The spacing between two neighbouring cilia is a in the x and y-directions, and their length L is set to 15 lattice unit (*lu*). Their motion is imposed to be in the (x,z) plane, and the MCW propagate in the x-direction only. Thus, cilia located at the same value of x beat in phase with each other. The ratio h/H between the PCL thickness and the height of the domain is set to 0.27 for

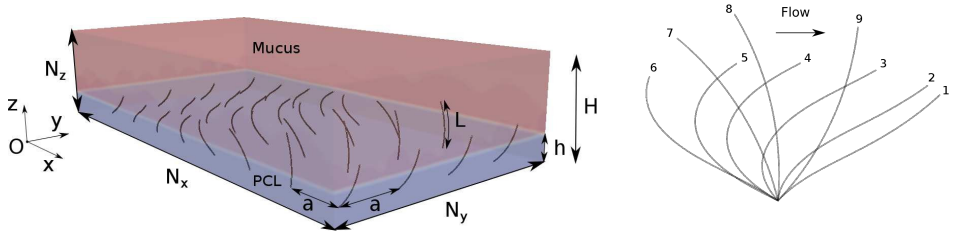

(a) (b)

FIGURE 1 – (a) Schematic view of the computational domain. The present case corresponds to an antipleptic MCW. The domain is filled with PCL (in blue) and mucus (in red). (b) Beating pattern of a cilium with the parametric equation used. Steps 1 to 6 correspond to the recovery phase, and steps 7 to 9 to the stroke phase.

all simulations. The equations of motion for the cilia are inspired from [5] and reproduce the beating pattern by resolving a 1D transport equation along a parametric curve. With such a beating pattern, the essential ingredients of the beating are captured, such as the angular amplitude between the beginning and the end of a stroke phase ($\theta = \frac{2\pi}{3}$), which agrees well with experimental data [7]. Figure 1(a) gives a schematic view of the geometry, and figure 1(b) an insight of the stroke and recovery phases as modeled in the present work.

In the simulations, the PCL thickness h varies between $0.6L$ to $0.9L$. Thus, the cilia tips enter the mucus phase when the cilia are in the stroke phase, as observed in real epithelium configurations. Both the PCL and the mucus are considered Newtonian fluids. The kinematic viscosity of the mucus is $\nu_m = 10^{-3}$ m^2/s, and the viscosity ratio $r_\nu = \nu_m/\nu_{PCL}$ between the mucus and PCL is set to 20. A recent study [8] has indeed shown that mucus transport was maximized for such viscosity ratios when considering a stiff transition between the mucus and PCL. The beating period of the cilia is $N_{it} \times dt$ (with $dt = 1$ using the classical LBM normalization), N_{it} being the number of iterations for a cilium to perform a complete beating cycle.

2.2 Algorithm

The numerical model is described in [9], and validated on several configurations involving flexible and moving boundaries in multiphase flows, with a 2^{nd} order accuracy.

The fluid part is first solved on a Cartesian grid with LBM using the Bhatnagar–Gross–Krook (BGK) model and a D3Q19 scheme. The collision and streaming steps proper to the LBM method are first performed. The model of [10] is used to simulate the two-phase flow as it allows to minimize the magnitude of spurious currents near the fluid-fluid interface. More importantly, it also enables to consider higher density or viscosity ratios. Then, values for the fluid velocity are interpolated at the Lagrangian points. It allows to compute an IB force to be spread onto the neighbouring Eulerian fluid nodes in order to ensure the no-slip condition along the cilia. The macroscopic fluid velocity is then updated.

Note that the geometric shape of the beating is fixed in all simulations. To save computing time, this shape is only computed once, decomposed into a finite number of steps (snapshots) during a beating period, and stored in memory. If necessary, an interpolation can be done in order to have the velocity values along the cilia in between two steps.

Since the model of [10] uses a Shan-Chen (SC) repulsive force [11], surface tension effects emerge intrinsically at the PCL-mucus interface.

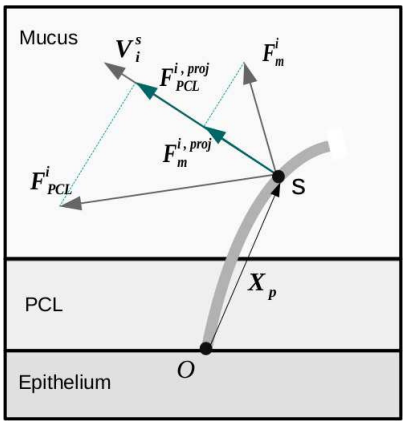

FIGURE 2 – Schematic view of a cilium with the corresponding forces exerted on the fluids. The interpolated IB forces applied by the i^{th} cilium onto the fluids - respectively $\boldsymbol{F}_m^i$ for the force imposed on the mucus phase and $\boldsymbol{F}_{PCL}^i$ for the force imposed on the PCL phase-, are projected on the velocity vector $\boldsymbol{V}_i^s$ corresponding to the s^{th} Lagrangian point. The lever arm is $L_p = \|\boldsymbol{X}_p \otimes \boldsymbol{V}_i^s\|/\|\boldsymbol{V}_i^s\|$.

Periodic boundary conditions are used in the x and y directions, while no-slip and free-slip boundary conditions are used at the bottom and top walls respectively. The size of the computational domain ranges from 50 *lu* to 400 *lu* depending on the configuration considered, except for the size along the z direction which is always set to 50 *lu*.

Taking advantage of the local character of the LBM algorithm, the code is parallelized using MPI libraries (Message Passing Interface), by splitting the full computational domain into 9 sub-domains of size $(N_x/3, N_y/3, N_z)$. More details on the numerical model can be found in [9].

2.3 Feedback law

The basic idea is to modulate the beating motion of the cilia as a function of the fluid motion. To do so, it is assumed that all cilia follow the same beating pattern, meanwhile a feedback of the fluids, which consists in accelerating or slowing down the motion of the cilia, is introduced.

Each cilium is discretized with $N_s = 20$ Lagrangian points. Let s be the subscript corresponding to the s^{th} Lagrangian point, starting from the base tip at $s = 1$, and $\boldsymbol{V}_i^s$ the velocity on the s^{th} Lagrangian point of the i^{th} cilium. For each cilium, we define the average velocity over all Lagrangian points $\boldsymbol{V}_i$, which is linked to the number of steps (snapshots) this cilium will skip during one iteration of the fluid solver. The fluid feedback onto the cilia thus consists in modifying the norm of the velocity vector $\|\boldsymbol{V}_i\|$, while its direction remains unchanged.

The feedback is computed in three steps. First, the IB forces corresponding to mucus and PCL are projected onto the corresponding velocity vectors for each Lagrangian point. Then, an estimate of the feedback is computed based on the torques of the forces for each Lagrangian point. Finally, the beating pattern of the cilia is adjusted at the beginning of the next time step. By doing so, only the norm of the velocity vector, but not its direction, is modified. A coupling parameter α is also introduced to control both the intensity of the fluid feedback and the direction of the wave propagation : $\|\mathbf{V}_i\| = \|\mathbf{V}_i\| \pm \alpha\|d\mathbf{V}_i\|$. Figure 2 gives a schematic view of the forces and variables considered. More details regarding the feedback law can be found in [12].

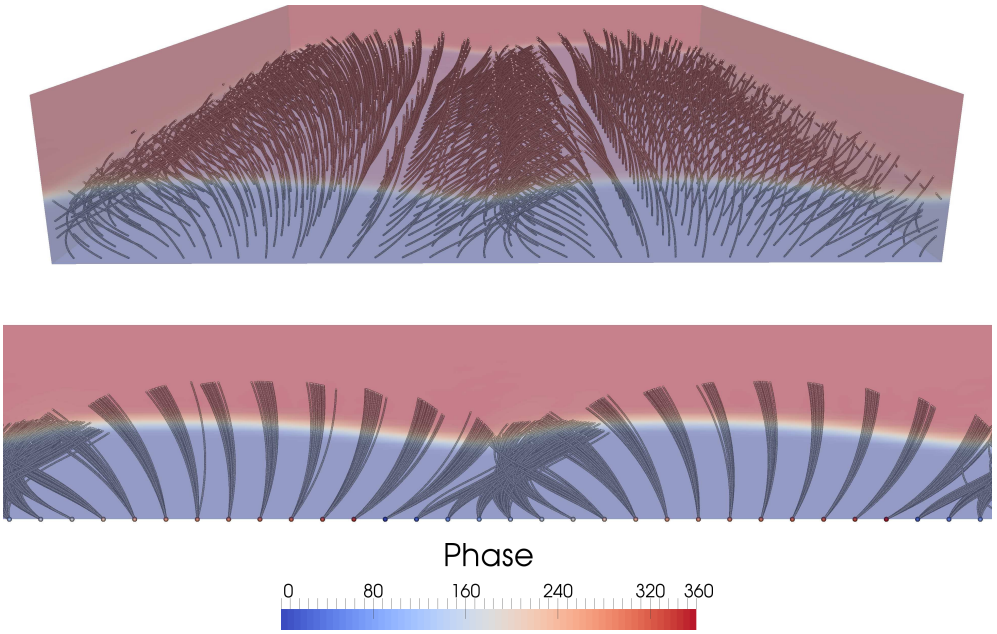

FIGURE 3 – Antipleptic MCW emerging from an initially random state of the cilia. 1024 cilia arranged in a 32×32 square are considered on a computational domain of size ($N_x = 161$, $N_y = 161$, $N_z = 32$) with a cilia spacing $a/L = 0.23$. The mucus phase is in red and the PCL phase in blue. The color bar indicates the phase of a particular cilium within one beating period, which is represented by a circle at its base. Top : 3D view of the system. Bottom : 2D view of the same system in a (x,y) plane to highlight the 3D modulation in the z-direction.

3. Results

3.1 Emergence of MCW

Using the feedback law previously introduced, both antipleptic and symplectic MCW are seen to emerge. The parameter α plays a role in the emergence : it controls both the direction of the wave propagation and the time for synchronization to occur (higher absolute values of α reduce the time for MCW to emerge). Figure 3 shows an antipleptic MCW emerging from cilia beating initially randomly, using $\alpha = -3.5$. In this figure the presence of two wavelengths can be noticed. The phase lag between neighbouring cilia is $\Delta\Phi = \pi/8$.

Moreover, assuming a least effort behaviour of the cilia (meaning $\alpha < 0$), antipleptic MCW are seen to emerge for small cilia spacings while symplectic MCW occur for higher cilia spacings (see figure 4). A tendency can also be observed (black line) and needs to be studied in more details. This result is important as it shows that natural cilia, who are usually highly packed, should adopt a least effort behaviour to organize in antipleptic MCW. However, with the present model, a least effort behaviour ($\alpha < 0$) induces a stroke phase longer than the recovery phase. On the contrary, assuming that the cilia beat faster when encountering a resistance (meaning $\alpha > 0$), the stroke phase becomes faster than the recovery phase as observed in real cilia configurations. While hydrodynamics interactions are sufficient to explain the synchronization of neighbouring cilia, they are not sufficient to explain the temporal asymmetry present in the beating pattern. Hence, the conclusion is that other biological parameters must also play a role. Note that the white space between the green and blue points (just above the black line) in figure 4 corresponds to simulations where no MCW emerged.

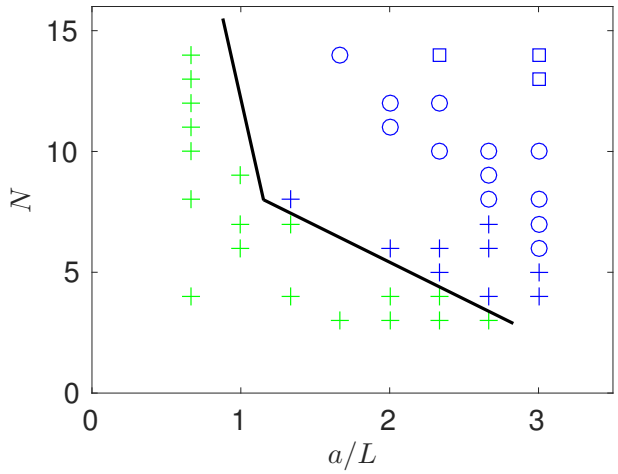

FIGURE 4 – Emergence of MCW as a function of the cilia spacing a/L and number N of cilia in a row. Green : Antipleptic MCW ; Blue : Symplectic MCW. The markers respectively represent : (+) : 1 wavelength ; (○) : 2 wavelengths ; and (□) : 3 wavelengths. The black line illustrates the presence of a "trend".

3.2 Transport efficiency of MCW

In order to quantify the efficiency of the MCW to transport fluids, a parametric study where the metachrony is imposed, has been performed. In the following, the stroke and recovery phases are fixed and take the same amount of time in order to study the influence of the spatial asymmetry only. Indeed, it is the only mechanism that is important for inducing motion in creeping flows [4]. In order to save CPU time, the results presented here have been obtained using a Reynolds number of 20 larger than the one usually seen for such configurations ($Re \approx 10^{-5}$). Thus, inertial effects are introduced in the model. However, it has been verified that such effects are small and do not modify the behaviour of MCW. The only notable quantitative differences are found for fully synchronized cilia : for such configurations, the inertial effects cancel the reversal of the flow that should occur during the recovery motion. More details regarding the effect of inertia can be found in [12].

The total volume of fluid displaced during a beating cycle for the different phase lags is compared in figure 5. For a small cilia spacing ($a/L = 1.67$), the efficiency of the antipleptic metachrony is obvious. It agrees well with the results of [17] who observed a larger net flow produced by antipleptic metachrony for this value of cilia spacing. Symplectic waves appear to be less or at best equally efficient than antipleptic motion, except for $\Delta\Phi = -7\pi/8$ for $a/L = 1.67$ where there is a peak in the total displaced volume of flow. There are two neighbouring maxima at $\Delta\Phi = \pi/4$ and $\Delta\Phi = \pi/2$ for $a/L = 1.67$ and $a/L = 2$ respectively, indicating that specific phase lags are more able to generate a strong flow.

A displacement ratio that will quantify the capacity of a given system to transport particles, with respect to a given amount of power, is now introduced. In that context, η_1 is defined by the mean fluid displacement over the x-direction during one beating cycle, divided by the mean power P^* that a cilium had to spend during this beating cycle. Since the main purpose of mucociliary clearance is to transport mucus, and since experimental data [13] report that the total thickness in the vertical direction of the mucus layer is in the range $[1.4L; 10L]$, values for the displacement were taken on an arbitrary plane $z/L = 3.2$ near the extremity of the domain. To obtain a value for the displacement, the instantaneous

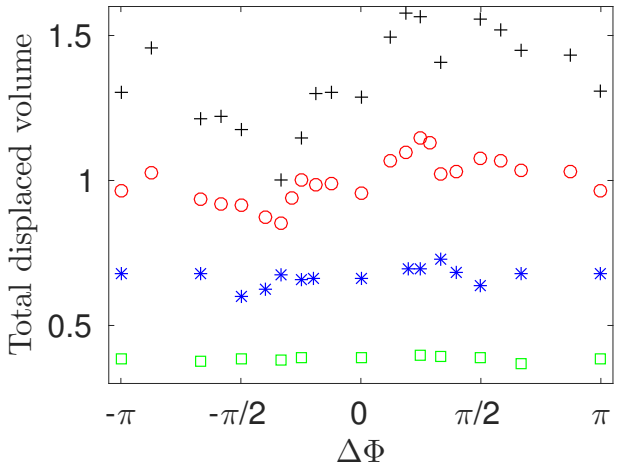

FIGURE 5 – Total dimensionless displaced flow volume generated by an array of cilia over a beating cycle for different phase lags and cilia spacings. + : $a/L = 1.67$; ◯ : $a/L = 2$; ∗ : $a/L = 2.53$; □ : $a/L = 3.33$.

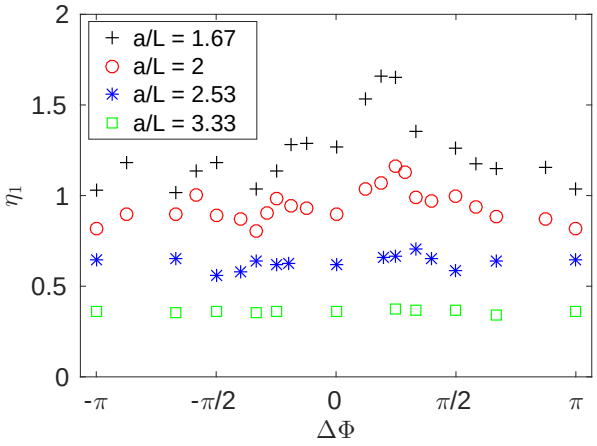

FIGURE 6 – Displacement ratio η_1 as a function of the phase lag $\Delta\Phi$ for different cilia spacings a/L.

average fluid velocity over the x-direction is computed, and the resulting value is then multiplied by the period of a full beating cycle, giving the mean displacement $< d_x >$ over one period on the (x,y,3.2L) plane. By dividing this mean displacement with appropriate quantities, a dimensionless expression of the displacement ratio is obtained : $\eta_1 = (< d_x > N_{cil})/(\lambda P^*)$, where N_{cil} is the number of cilia and λ the metachronal wavelength. For the synchronized case, i.e. $\Delta\Phi = 0$, λ is infinite and thus the size of the domain over the x direction was used and divided by the number of cilia.

On Figure 6, one can see the displacement ratio η_1 for different cilia spacings a/L and phase lags $\Delta\Phi$. A clear peak exists for the smaller cilia spacing ($a/L = 1.67$) for a phase lag $\Delta\Phi = \pi/4$, showing that such antipleptic MCW are more able to transport fluids. On the other hand, symplectic MCW are often less, or at best equally efficient, than antipleptic MCW.

The mixing capacity of the systems has also been evaluated. To do so, the average stretching rate during a beating period has been computed. Figure 7 shows the corresponding results. One can see that the antipleptic MCW corresponding to $\Delta\Phi = \pi/4$ and $a/L = 1.67$ present the best capacity for stretching

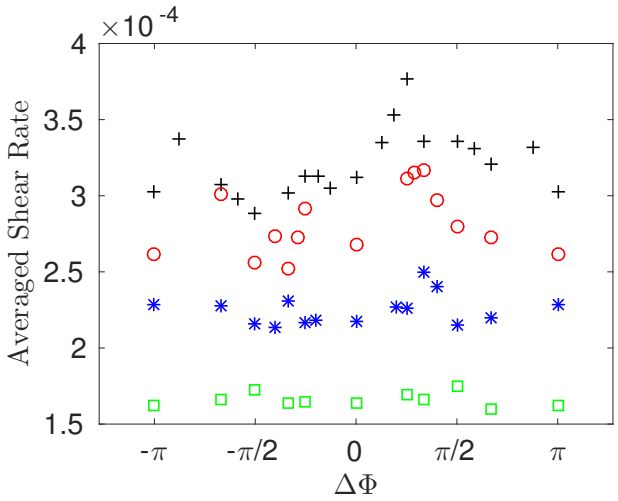

FIGURE 7 – Average stretching rate computed between $0 < z < 1.4L$ as a function of the phase lag $\Delta\Phi$ for different cilia spacings a/L.

the fluids. A more complete study is ongoing.

4. Conclusion

Considering a simple feedback law, both antipleptic and symplectic MCW were observed to emerge spontaneously in a two-layer environment. Considering a least effort behaviour for cilia, antipleptic MCW were obtained for the smallest cilia spacing studied, while symplectic MCW were observed for larger ones. The resulting beating pattern consisted in a slow stroke phase and a fast recovery phase, which is the opposite of what is observed in nature. Hence, other biological parameters must play a role in the cilia beating pattern, and hydrodynamic interactions are not sufficient to fully explain their motion. A parametric study has also been performed and shows that the antipleptic MCW with $\Delta\Phi = \pi/4$ are the most efficient in transporting and mixing fluids.

5. Acknowledgment

The authors would like to thank the Natural Sciences and Engineering Research Council of Canada for its financial support through a Discovery Grant (RGPIN-2015-06512). This work was granted access to the HPC resources of Compute Canada and Aix-Marseille University (project Equip@Meso ANR-10-EQPX-29-01).

Références

[1] J.H. Widdicombe, J.G. Widdicombe, Regulation of human airway surface liquid, Resp. Physiol., 99(1) (1995) 3–12.

[2] O. Lafforgue, S. Poncet, I. Seyssiecq-Guarente, J. Favier, Rheological characterization of macromolecular colloidal gels as simulant of bronchial mucus, 32^{nd} International Conference of the Polymer Processing Society (PPS-32), Lyon, France, 25-29 July 2016.

[3] S.K. Lai, Y.Y. Wang, D. Wirtz, J. Hanes, Micro- and macrorheology of mucus, Adv. Drug Deliver. Rev., 61(2) (2009) 86–100.

[4] S.N. Khaderi, M.G.H.M. Baltussen, P.D. Anderson, J.M.J. Den Toonder, P.R. Onck, Breaking of symmetry in microfluidic propulsion driven by artificial cilia, Phys. Rev. E, 82 (2010) 027302.

[5] R. Chatelin, Méthodes numériques pour l'écoulement de Stokes 3D : fluides à viscosité variable en géométrie complexe mobile ; application aux fluides biologiques, PhD thesis, Institut de Mathématiques de Toulouse, 2013.

[6] M.A. Sleigh, The biology of Cilia and Flagella, Pergamon Press, Oxford, 1962.

[7] M.A. Sleigh, J.R. Blake, N. Liron, The Propulsion of Mucus by Cilia, Am. Rev. Respir. Dis., 137(3) (1988) 726–741.

[8] R. Chatelin, P. Poncet, A parametric study of mucociliary transport by numerical simulations of 3D non-homogeneous mucus, J. Biomech., 49 (2016) 1772–1780.

[9] Z. Li, J. Favier, U. D'Ortona, S. Poncet, An improved explicit immersed boundary method to couple with Lattice Boltzmann model for single- and multi-component fluid flows, J. Comput. Phys., 304 (2016) 424–440.

[10] M.L. Porter, E.T. Coon, Q. Kang, J.D. Moulton, J.W. Carey, Multicomponent interparticle-potential lattice Boltzmann model for fluids with large viscosity ratios, Phys. Rev. E, 86 (2012) 036701.

[11] X. Shan, H. Chen, Simulation of nonideal gases and liquid-gas phase transitions by the lattice Boltzmann equation, Phys. Rev. E, 49(4) (1994) 2941–2948.

[12] S. Chateau, J. Favier, U. D'Ortona, S. Poncet, Transport efficiency of metachronal waves in 3D cilia arrays immersed in a two-phase flow, (HAL, hal-01494742, `https://hal.archives-ouvertes.fr/hal-01494742`), J. Fluid Mech.

[13] S.L. Winters, D.B. Yeates, Roles of hydration, sodium, and chloride in regulation of canine mucociliary transport system, J. Appl. Physiol., 83(4) (1997) 1360–1369.

[14] S. Gueron, K. Levit-Gurevich, Energetic considerations of ciliary beating and the advantage of metachronal coordination, PNAS, 96(22) (1999) 12240–12245.

[15] J. Elgeti, G. Gompper, Emergence of metachronal waves in cilia arrays, PNAS, 110(12) (2013) 4470–4475.

[16] S.M. Mitran, Metachronal wave formation in a model of pulmonary cilia, Comput. Struct., 85(11–14) (2007) 763–774.

[17] S. N. Khaderi, J. M. J. Den-Toonder, P. R. Onck, Microfluidic propulsion by the metachronal beating of magnetic artificial cilia : a numerical analysis, J. Fluid Mech., 688 (2011) 44–65.